Front. Chem. Sci. Eng. 2023, 17(6): 749–758
https://doi.org/10.1007/s11705-022-2261-0

RESEARCH ARTICLE

Highly selective and green recovery of lithium ions from lithium iron phosphate powders with ozone

Ruiqi Li, Kang Li, Wei Wang, Fan Zhang, Shichao Tian, Zhongqi Ren (✉), Zhiyong Zhou (✉)

State Key Laboratory of Chemical Resource Engineering, Beijing University of Chemical Technology, Beijing 100029, China

Abstract Since lithium iron phosphate cathode material does not contain high-value metals other than lithium, it is therefore necessary to strike a balance between recovery efficiency and economic benefits in the recycling of waste lithium iron phosphate cathode materials. Here, we describe a selective recovery process that can achieve economically efficient recovery and an acceptable lithium leaching yield. Adjusting the acid concentration and amount of oxidant enables selective recovery of lithium ions. Iron is retained in the leaching residue as iron phosphate, which is easy to recycle. The effects of factors such as acid concentration, acid dosage, amount of oxidant, and reaction temperature on the leaching of lithium and iron are comprehensively explored, and the mechanism of selective leaching is clarified. This process greatly reduces the cost of processing equipment and chemicals. This increases the potential industrial use of this process and enables the green and efficient recycling of waste lithium iron phosphate cathode materials in the future.

Keywords lithium iron phosphate powder, stoichiometric number, selective leaching, lithium recovery

1 Introduction

The rapid development of electric vehicles is important for improving the energy structure [1] and can effectively alleviate the greenhouse effect [2]. The use of lithium-ion batteries (LIBs) as power sources for electric vehicles is also flourishing [3]. It has been reported that in 2018, in China alone, more than 1.25 million new-energy vehicles were produced, and production reached 2 million by 2020 [4]. This trend will inevitably lead to production of a large number of spent LIBs [5]. Lithium iron phosphate ($LiFePO_4$, LFP) is widely used as a battery material because of its low preparation cost, high safety, and good cycling performance [6,7]. The recycling of spent LFP batteries is necessary. The toxic materials in LIBs adversely affect the environment [8] and human health [9], and recovery of the lithium in LFP can effectively alleviate the problem of scarce lithium resources [10–12]. Unlike the $LiNi_{1-x-y}Co_xMn_yO_2$ series of LIBs, those based on LFP do not contain other high-value metals, therefore more research has been performed on the recycling of $LiNi_{1-x-y}Co_xMn_yO_2$ batteries [13–15] than on LFP recycling. Research on the recycling of spent LFP batteries is therefore important.

In recent years, LFP recycling has mainly been achieved by using direct regeneration [16,17] and hydrometallurgical methods [18]. Direct regeneration is simple, but the performances of the regenerated electrodes are worse than those of commercial products [19]. Hydrometallurgical methods have the advantages of a mild reaction, and high metal leaching, recovery efficiency, and product purity [20]. LFP has a stable structure and properties [21], therefore the use of selective recovery methods has been proposed [5,22]. Such methods promote selective leaching of lithium into the solution, and retention of iron in the leaching residue. This method shortens the operating process compared with that used in traditional hydrometallurgical methods, which decreases the amount of leaching agent, and generates economic benefits from the recycling of spent LFP cathode materials. Table 1 summarizes the current research on selective recovery of lithium from spent LFP cathode materials. Li et al. [23] used a stoichiometric H_2SO_4–H_2O_2 system. The lithium leaching yield was 96.9%, whereas the iron leaching yield was only 0.027%. These results showed that precise control could be achieved by using this system, but the leaching mechanism was not studied. Jing et al. [24] studied the redox potential-pH relationship in a Li–Fe–P–H_2O system at 298–473 K and reported that the lithium in LFP could be leached into solution at an appropriate pH and redox potential. In their subsequent research [25], they

Received July 18, 2022; accepted September 19, 2022

E-mails: renzq@mail.buct.edu.cn (Ren Z.), zhouzy@mail.buct.edu.cn (Zhou Z.)

Table 1 Reported selective recoveries in recycling of LFP cathode materials

Year	Reagent	Leaching condition	Leaching yield/%	Ref.
2017	H_2SO_4 (0.3 mol·L^{-1}) + H_2O_2	Li:H_2SO_4:H_2O_2 (mol/mol/mol) = 1:0.57:2.07, T = 60 °C, t = 120 min	Li: 96.85, Fe: 0.03	[23]
2018	CH_3COOH (0.8 mol·L^{-1}), H_2O_2 (6 vol %)	S/L = 120 g·L^{-1}, T = 50 °C, t = 30 min	Li: 95.05, Fe: 0.10	[28]
2018	$C_2H_2O_4$ (0.3 mol·L^{-1})	S/L = 60 g·L^{-1}, T = 80 °C, t = 60 min	Li: 98.00, Fe: 8.00	[29]
2018	$Na_2S_2O_8$	Li:$Na_2S_2O_8$ (mol/mol) = 2:1.05, S/L = 300 g·L^{-1}, T = 25 °C, t = 20 min	Li: 99.00, Fe: 0.05	[25]
2019	NaCl	LFP:NaCl (g/g) = 1:2	Li: > 90.00, Fe: < 1.00	[26]
2020	$Fe_2(SO_4)_3$	$Fe_2(SO_4)_3$:LFP (mol/mol) = 1:2, T = 28 °C, t = 30 min, S/L = 500 g·L^{-1}	Li: 97.00	[27]
2020	$Na_2S_2O_8$, H_2SO_4 (0.3 mol·L^{-1})	Li:$Na_2S_2O_8$ (mol/mol) = 0.45, L/S = 11.1 mL·g^{-1}, T = 60 °C, t = 1.5 h	Li: 97.55, Fe: 1.39	[30]
2022	H_2O_2	S/L = 10 g·L^{-1}, T = 50 °C, t = 30 min	Li: 97.60, Fe: < 1.00	[31]

used $Na_2S_2O_8$ to achieve complete selective leaching of lithium from spent LFP cathode materials. However, the Na_2SO_4 produced in the process affected subsequent lithium recovery. Liu et al. [26] used a mechanochemical method to replace LFP with NaCl as an auxiliary agent, and achieved selective leaching of lithium in an acid-free environment. However, the processing time of up to 6 h greatly reduced the processing efficiency. The NaCl used in the process was leached into the leaching solution during leaching, and this affected subsequent recovery of lithium. Dai et al. [27] used $Fe_2(SO_4)_3$ to achieve selective recovery of lithium. The leaching process was rapid and acid free, and the $Fe_2(SO_4)_3$ could be recycled. However, the recovery of $Fe_2(SO_4)_3$ required the use of NaOH as a precipitant, and the $Fe_2(SO_4)_3$ contaminated the leachate. It is therefore important to find a greener and purer selective leaching system for the efficient recovery of lithium from spent LFP cathode materials.

In this study, we used HCl as the leaching agent and ozone as the oxidant for selective leaching of lithium from LFP powders. As a strong oxidant, ozone has an oxidation−reduction potential of 2.07 eV under an acidic environment. Ozone can be prepared *in situ* with air or oxygen as the raw material, and the decomposition product is oxygen. Using ozone as an oxidant can greatly reduce the problem of high-salt wastewater and exhaust gas emissions. Compared with traditional hydrogen peroxide [31] as an oxidant, there is no transportation and storage safety problem, and it is inexpensive and easy to obtain. Although H_2O_2 as an oxidant shows good selectivity, H_2O_2 is easily decomposed at high temperature. Therefore, using ozone as an oxidant has certain advantages compared with other leaching systems. The optimal leaching conditions were explored, and a two-stage leaching process was proposed based on characterization and verification experiments. High-purity Li_2CO_3 was prepared from the leaching solution.

2 Experimental

2.1 Materials

LFP powder with the major element contents (38.05 wt % Fe and 4.66 wt % Li) was purchased from the Huawei Ruike Chemical Co., Ltd. (Beijing, China). HCl (36–38 wt %), NaOH, and Na_2CO_3 were purchased from the Beijing Chemical Plants (Beijing, China). A 3S-T10 ozone generator supplied by Beijing Tonglin Technology Co., Ltd. (Beijing, China) was used to produce ozone at the required concentrations from pure oxygen.

2.2 Selective leaching of lithium

The powders and HCl (total 8 g) were placed in a 250 mL three-necked flask and ozone was fed into the solution. Taking oxygen as the gas source, the output ozone concentration is adjusted by adjusting the power of the ozone generator, and monitored by ozone concentration analyzer (3S-J5000). Ozone is fully contacted with the leaching solution through titanium alloy aeration head (pore size 1–2 μm), and the temperature during the reaction is controlled by a circulating water machine (SHB-III). The reaction was performed for 60 min at 20 °C.

After the reaction was complete, the solution was filtered. Atomic absorption spectroscopy (AA-6880, Shimadzu, Japan) was used to determine the concentrations of Li and Fe in the leachate. The leaching yield η_i of various elements was calculated by using Eq. (1):

$$\eta_i = \frac{c_i V}{m\omega_i} \times 100\% \tag{1}$$

where c_i (g·L^{-1}) is the concentration of element i (i = Li, Fe); V (L) is the volume of leachate; and m (g) and ω_i are the mass and the quality score of element i in the initial LFP powder.

To further study the iron leaching process, Fe^{2+} was titrated with $K_2Cr_2O_7$ to determine the ratio of Fe^{2+} to Fe^{3+} in the leaching solution at different leaching times.

Take 2 mL of the solution, add 10 mL of phosphorus-sulfur mixed acid, add H_2O to 100 mL, drop in sodium diphenylamine sulfonate indicator, use $K_2Cr_2O_7$ for titration, and titrate until the solution is purple, which is the end point. The ferrous iron concentration was calculated using Eq. (2):

$$C_{Fe^{2+}} = \frac{C_{\frac{1}{6}K_2Cr_2O_7} \times V \times 55.84}{2}, \tag{2}$$

where V (mL) is the volume of titrant consumed; $C_{Fe^{2+}}$ ($g \cdot L^{-1}$) is the concentration of ferrous iron in the solution to be tested.

The calculation of purity was carried out by weighing a certain mass of Li_2CO_3 product, dissolving them in a certain volume of solution and using atomic absorption spectroscopy to determine the concentration of Li ion in the solution after the dissolution was complete. The purity of the Li_2CO_3 product was obtained by the ratio of the actual concentration to the theoretical concentration.

The mechanisms of leaching and oxidation were investigated by performing X-ray diffraction (XRD) on solid samples of the initial LFP and the leaching residue over the 2θ 5°–90°. The Fe valences were identified by X-ray photoelectron spectroscopy (XPS). The surface morphologies were examined by scanning electron microscopy (SEM). Dynamic light scattering was used to determine the particle size distributions of the initial LFP and the leaching residue.

3 Results and discussion

The redox potential of ozone in an acidic environment is 2.07 eV, second to fluorine. The reaction of LFP with ozone in HCl is shown in Eq. (3):

$$2LiFePO_4 + O_3\uparrow + 2HCl \rightarrow 2LiCl + 2FePO_4 + H_2O + O_2\uparrow \quad (3)$$

The effects of various parameters on the leaching yields of Li and Fe ions were studied.

3.1 Effects of concentration and total amount of HCl

Figure 1 shows that when molar ratio of H to Li = 0.9, 90% of the total amount of lithium can theoretically be leached. The leaching yields achieved at different HCl concentrations were 71.6%–87.63%, i.e., basically the theoretical value. The leaching yield of iron was less than 0.01%, which shows that the system gives good selective leaching. When H/Li (mol/mol) = 1, the HCl leaching yield at 0.3 $mol \cdot L^{-1}$ was 98.38%. The lithium leaching yield decreased with increasing HCl concentration. This is mainly because when the total amount of acid is the same, the greater the acid concentration, the smaller the volume of HCl required, the shorter the contact time with ozone, and the shorter the residence time of ozone. This decreases the effective usage rate of ozone and reduces the leaching yield. With further increases in the total amount of HCl, the lithium leaching yield also increases, and can reach 96%–98%, i.e., complete leaching of lithium can basically be achieved. For iron, when H/Li (mol/mol) = 0.9, the iron leaching yield did not change with changes in the acid concentration, and the leaching yield was less than 0.01%. When H/Li (mol/mol) = 1, the iron leaching yield was as high as 0.96%, which is much higher than the yields at other concentrations. This is mainly because the volume of 0.3 $mol \cdot L^{-1}$ solution is larger than those at other concentrations and more iron can be dissolved. When H/Li (mol/mol) was increased to 1.1, the iron leaching yield rapidly increased to more than 5%. This is mainly because of the excess HCl in the system, which does not participate in the reaction and dissolves iron. When the concentration was increased to 0.6 $mol \cdot L^{-1}$, the Fe leaching yield was much higher than those at other HCl concentrations. This indicates that the iron leaching yield is affected by both the concentration and total amount of acid. Although the Lithium leaching yield in 0.3 $mol \cdot L^{-1}$ HCl reached 98.38%, the iron leaching yield was as high as 0.96%. At the same time, the use of low-concentration acid increases the volume of the solution and increases the cost of subsequent treatment. Although the lithium leaching yield in 0.4 $mol \cdot L^{-1}$ HCl was only 94.48%, the iron leaching yield was only 0.037%, therefore, considering the effects on leaching of Li and Fe, and the cost of subsequent treatment, 0.4 $mol \cdot L^{-1}$ HCl and H/Li (mol/mol) = 1 were selected for subsequent experiments.

3.2 Effect of ozone concentration

Ozone is the oxidant in the leaching process and the key

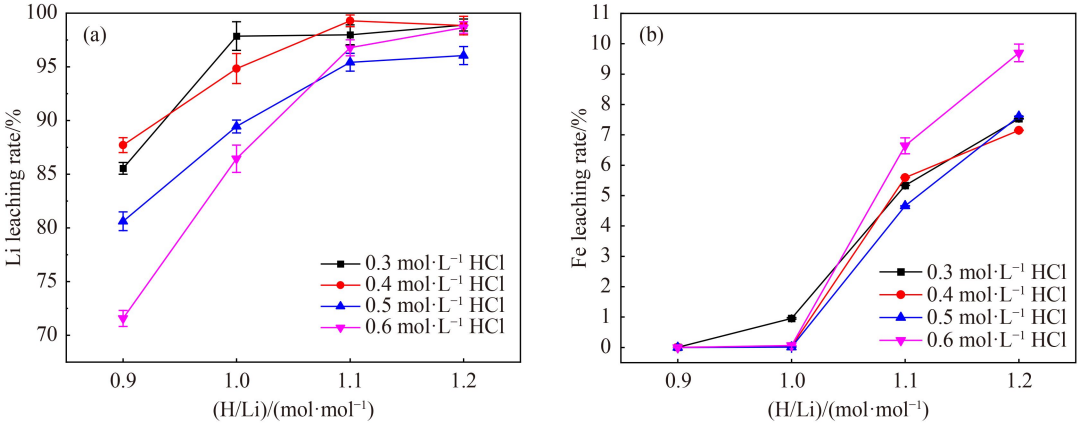

Fig. 1 Effects of concentration and total amount of HCl on leaching yields of (a) Li and (b) Fe ions.

to achieving selective leaching. The ozone concentration determines the number of ozone molecules that can effectively participate in the reaction per unit time. The results in Fig. 2 show that when the ozone concentration was increased to 10 ± 1 mg·L^{-1}, the lithium leaching yield reached 99.84% in 1 h. When the ozone concentration was further increased, the lithium leaching yield in 1 h could exceed 99%, and the iron leaching yield was only 0.048%. The time required for lithium leaching to reach equilibrium was shortened, and almost complete leaching was achieved in 40 min. Iron leaching involves two stages: rapid leaching at 0–20 min, and slow leaching at 30–60 min. This is mainly because ozone was continuously fed in during the reaction, and there was excess HCl. As the reaction progressed, the HCl was consumed, and the iron leaching yield gradually decreased. Figure 2 clearly shows that the initial iron leaching yield is the highest. The leaching yield gradually decreased with increasing leaching time. This is because there is initially an excess of HCl, and ozone was continuously introduced during the reaction. When there is insufficient oxidant, iron dissolves in the HCl. As the amount of oxidant increased, the leached ferrous iron was oxidized and precipitated, therefore the iron leaching yield gradually decreased. As the concentration continued to increase, the iron leaching yield basically became stable. Considering the leaching effect and the cost of ozone, all subsequent experiments were performed with an ozone concentration of 10 ± 1 mg·L^{-1}.

3.3 Effect of ozone penetration rate

The ozone concentration and the inflow rate jointly determine the total amount of ozone. The gas velocity determines the degree of gas–liquid mixing. The greater the gas velocity, the greater the contact among HCl, ozone, and LFP. Figure 3 shows that when the ozone penetration rate was 0.5 L·min^{-1}, although the ozone concentration was 10 ± 1 mg·L^{-1}, the ozone penetration rate was insufficient and the lithium leaching yield was only 89% in 1 h. Because there was insufficient oxidant, the iron leaching yield was as high as 3.213%. When the ozone penetration rate was increased to 1.5 L·min^{-1}, the lithium leaching yield reached 99.81% after 1 h, and the iron leaching yield was only 0.07%. The time required for lithium leaching to reach equilibrium became shorter. When the inflow rate was 1.5 L·min^{-1}, it takes 50 min to reach equilibrium, and when the inflow rate was 2 L·min^{-1},

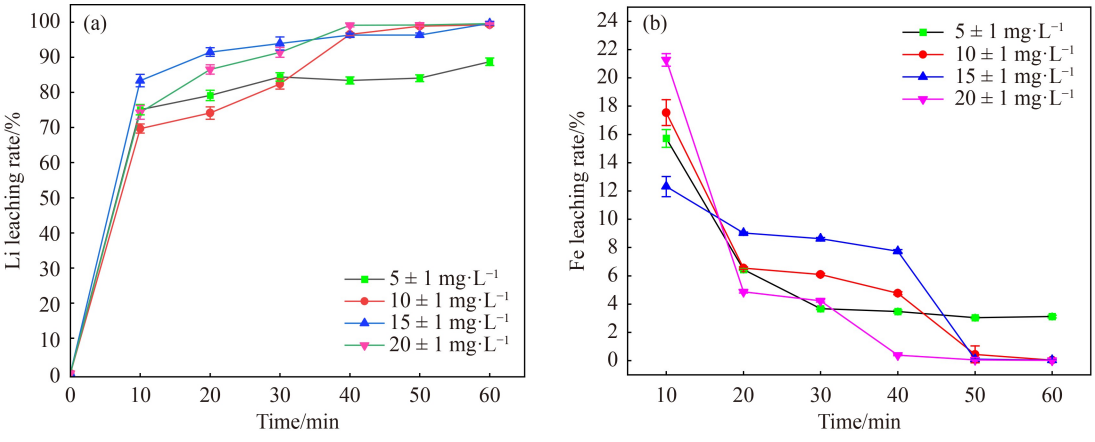

Fig. 2 Effect of ozone concentration on leaching yields of (a) Li and (b) Fe ions.

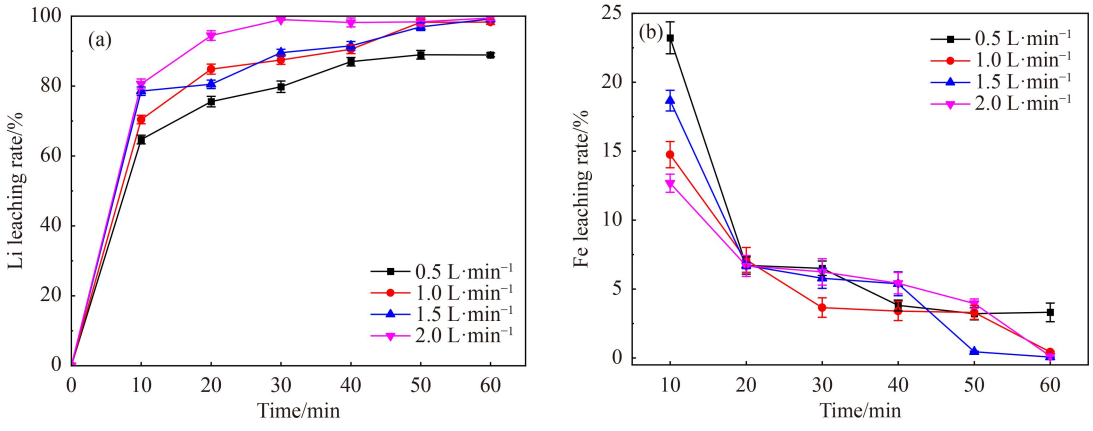

Fig. 3 Effect of ozone penetration rate on leaching yields of (a) Li and (b) Fe ions.

it only taken 30 min. However, the iron leaching yield in 1 h did not continue to decrease at high gas velocities. Considering the lithium and iron leaching effects, and the cost and energy consumption of ozone production, 1.5 L·min^{-1} was selected for subsequent experiments.

3.4 Effect of temperature

The solubility of ozone in water is 10 times that of oxygen under the same conditions; its dissolution is related to factors such as pressure, temperature, and the solution pH [32]. The solubility decreases with increasing solution temperature, and this affects the half-life and stability. Figure 4 shows that the lithium leaching yield was greater than 99% after leaching for 1 h at 10–40 °C, and the iron leaching yield was less than 0.5%. This is mainly because the continuous introduction of ozone into the reaction led to oxidation of Fe^{2+} to Fe^{3+}. When ozone was introduced, it participated in the reaction; the temperature had almost no effect on its decomposition, and therefore had no effect on the leaching yields of Li and Fe ions. The temperature mainly affected the time required for lithium leaching to reach equilibrium during the process. Metal leaching is essentially endothermic, and a high reaction temperature creates thermodynamically favorable conditions during leaching [33]. The time required for lithium leaching to reach equilibrium decreased with increasing temperature. At 10 and 20 °C, it takes 50 min to reach leaching equilibrium. When the temperature was 30 °C, it takes only 40 min to achieve equilibrium, and when it was increased to 40 °C, it taken only 30 min. These results are consistent with those reported when H_2O_2 [28] was used as the oxidant. This indicates that increasing the temperature increases the reaction rate. The temperature initially had a significant effect on the iron leaching yield, but after leaching for 1 h the leaching yields were all less than 0.5%. This system can therefore achieve complete selective leaching of lithium at low temperatures, which means that production can be performed at room temperature (15–25 °C) throughout the year, which greatly reduces energy consumption and production costs.

3.5 Recovery of lithium in leachate

Under the optimal operating conditions, i.e., 0.4 mol·L^{-1} HCl, Li:H (mol/mol) = 1:1, ozone concentration 10 ± 1 mg·L^{-1}, and ozone penetration rate 1.5 L·min^{-1}, the lithium and iron leaching yields reached 98.81% and 0.07%, respectively, after leaching at 20 °C for 60 min. After leaching was complete, a colorless and transparent filtrate was obtained by suction filtration, and lithium was present in solution in the form of LiCl. The leaching solution was concentrated. During this process, the solution gradually turned yellow. Then NaOH was added to adjust the pH to 9–10 to remove trace amounts of iron in the solution. Suction filtration gave a colorless and transparent filtrate. Addition of solid Na_2CO_3 at a Li^+:CO_3^{2-} molar ratio of 2:1.1, heating at 95 °C for 2 h, and suction filtering gave a white Li_2CO_3 precipitate. The precipitate was washed with boiling deionized water, and placed in a vacuum drying oven at 120 °C for 12 h (Fig. S1, cf. Electronic Supplementary Material, ESM). The primary precipitation yield of Li_2CO_3 was 89%, and the purity of the obtained Li_2CO_3 was 99.9%. This meets the requirement for battery-grade Li_2CO_3 and the product can therefore be used as a raw material for LIBs. The leaching residue was examined by XRD. Figure S2 (cf. ESM) shows that the XRD pattern of the recovered Li_2CO_3 matches the standard Li_2CO_3 pattern.

3.6 Recovery of leaching residue

After the leaching process was complete, the filtrate obtained by suction filtration was used for lithium recovery. The obtained leaching residue mainly consists of C, Fe, P and O elements was washed several times with deionized water and dried in a vacuum drying oven

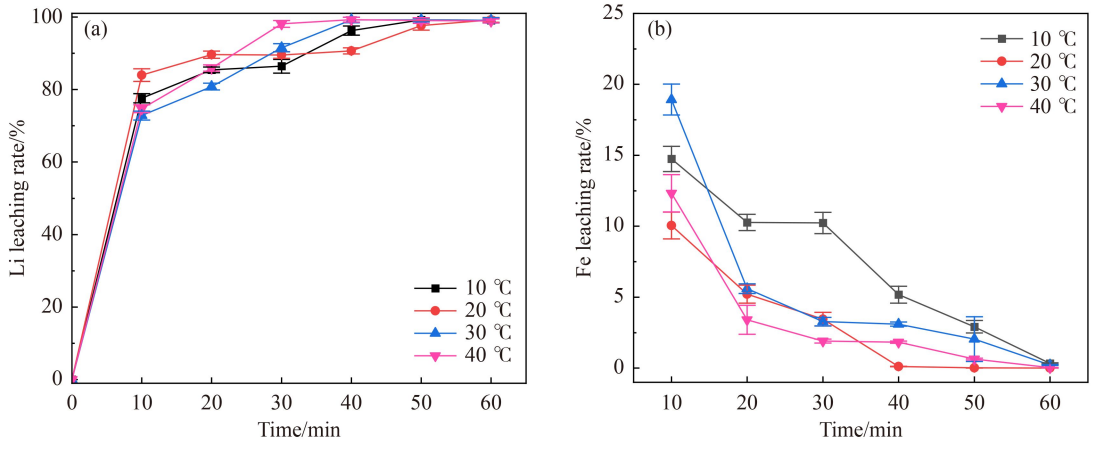

Fig. 4 Effect of temperature on leaching yields of (a) Li and (b) Fe ions.

at 60 °C for 12 h. The obtained product containing few LFP and conductive carbon and abundant $FePO_4$ is shown in Fig. S3 (cf. ESM). The conductive carbon can be separated by magnetic separation. The product was examined by XRD. Figure S4 (cf. ESM) shows that the peaks in the XRD pattern of the product are in good agreement with those in the $FePO_4$ pattern. This indicates that the iron remains in the leaching residue in the form of $FePO_4$ and the purity of $FePO_4$ is very high. This process therefore achieves selective leaching of lithium.

3.7 Investigation of leaching process and mechanism

The experimental results show that the trend in the iron leaching yield during the leaching process can be divided into two parts. In the first part, at 0–20 min, leaching was rapid. In the second part, at 30–60 min, leaching was slow. This was used as a basis for clarification of the leaching mechanism. First, the roles of HCl and ozone, and the synergy between them, were investigated. Three sets of control experiments were performed: leaching experiments with HCl, leaching experiments with ozone, and leaching experiments with HCl and ozone combined. The experimental results are shown in Fig. 5.

Figure 5 shows that in leaching with HCl alone, the lithium and iron leaching yields reached equilibrium within 10 min. The leaching yield of lithium was about 50%, and that of iron was about 34%. When ozone alone was used for leaching, almost no iron was leached (< 0.1%) and the lithium leaching yield in 60 min was only 3.75%. This shows that although ozone has strong oxidizing properties, it cannot oxidize Fe^{2+} to Fe^{3+} in a neutral environment because of the stable crystal structure of LFP materials. The lithium and iron leaching yields therefore remain at low levels. When HCl-ozone was used for leaching, the lithium leaching yield reached 53.91% after 2 min, and leaching equilibrium was basically reached after 40 min; the leaching yield was 99.35%. The iron leaching yield was consistent with the previous experimental results. According to Eq. (3), the leaching process consumes HCl. The solubilities of LFP and $FePO_4$ in HCl decrease with increasing HCl consumption, and this decreases the iron leaching yield. The concentrations of HCl at various reaction times were determined by titration with 0.1 $mol \cdot L^{-1}$ NaOH solution; the results are shown in Fig. S5 (cf. ESM).

Figure S5 shows that the trend in the H^+ concentration is consistent with the trends in the lithium and iron leaching yields; the leaching process can be divided into rapid and slow leaching processes. At the end of the reaction, the H^+ concentration was only 0.012 $mol \cdot L^{-1}$. This shows that in an acidic environment, ozone oxidizes the Fe^{2+} in LFP to Fe^{3+}, which is consistent with Eq. (3). The solubilities of LFP and $FePO_4$ at 20 °C in 0.01–0.4 $mol \cdot L^{-1}$ HCl are shown in Table 2. The data in Table 2 show that as the concentration of HCl increases, the solubilities of LFP and $FePO_4$ also increase. The solubility of LFP in HCl is much greater than that of $FePO_4$ under the same conditions. The iron leaching process was further studied by using $K_2Cr_2O_7$ to titrate Fe^{2+} at different reaction times to determine the Fe^{2+}:Fe^{3+} ratio in the leaching solution at different leaching times.

The difference method was used to obtain the concentrations and total amounts of Fe^{2+} and Fe^{3+} in the

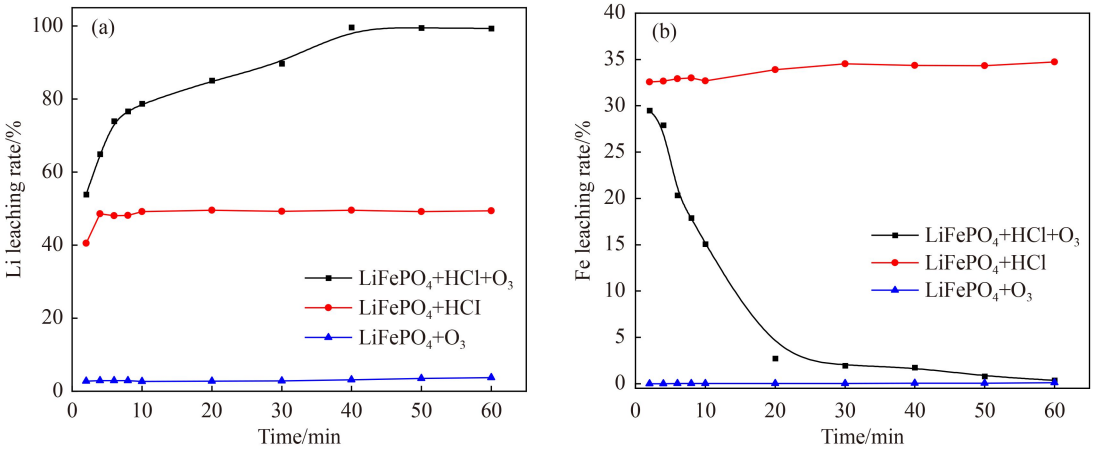

Fig. 5 Effect of different experimental conditions on leaching yields of (a) Li and (b) Fe ions.

Table 2 Solubilities of LFP and $FePO_4$ in HCl of different concentrations at 20 °C

Solution	C(HCl)/($mol \cdot L^{-1}$)					
	0.01	0.05	0.10	0.20	0.30	0.40
LFP g/100 g HCl solution	0.0040	0.1302	0.5067	1.0563	1.8273	2.4257
$FePO_4$ g/100 g HCl solution	0.00003	0.0001	0.0002	0.0005	0.0018	0.0038

leaching solution at different leaching times, and the Fe^{2+}:Fe^{3+} ratios in the leaching solution at different reaction times were calculated; the results are shown in Fig. 6. Clearly, the iron leaching yield dropped rapidly from 29.50% to 2.722% within the first 20 min. In this process, the proportion of Fe^{2+} in the leaching solution was greater than 90%, which means that within 0–20 min the Fe^{2+} in the crystal lattice was directly oxidized to Fe^{3+} under the combined effects of HCl and ozone. Lithium was leached into the solution. At the same time, the solubility of LFP decreased with increasing HCl consumption, which decreased the total iron leaching yield. Starting from 30 min, the proportion of Fe^{3+} in the leaching solution rapidly rose to 68%. At 50 min, the Fe^{3+} content rose to 100%. This shows that in the slow oxidation process, which occurred at 30–60 min, the oxidation of Fe^{2+} in the LFP was completed, and the product was retained in the leaching residue in the form of $FePO_4$.

Thermodynamic equilibrium can determine whether the reaction can proceed spontaneously, which can provide guidance for the selective leaching of lithium ions from LFP cathode materials [34]. Since the leaching reaction is carried out in solution, during the thermodynamic calculation of the leaching process, the main focus point is on the relevant chemical reactions occurring in the range of the potential lines of O_2 ($O_2\uparrow + 4H^+ + 4e^- = 2H_2O$) and H_2 ($2H^+ + 2e^- = H_2\uparrow$) [35,36].

The detailed E-pH formula and the relevant equilibrium reaction formula of Li–Fe–P–H_2O at 298.13 K are shown in Tables S1 and S2 (cf. ESM). It can be clearly seen from the Fig. 7 that when the pH is lower than 0.6, Fe ion exists in the form of Fe^{3+} at high potential and in the form of Fe^{2+} at low potential. When the pH of the solution is close to 7, Fe ion exists in the form of several forms of hydroxide precipitation, including $Fe(OH)_3$ at high potential and $Fe(OH)_2$ at low potential. Therefore, in order to realize the transformation from LFP to $FePO_4$, both suitable acid concentration and certain redox potential are required.

The traditional acid leaching method is to leach all the metal ions in the LFP according to the black arrow path, and then oxidize Fe^{2+} to Fe^{3+} to form precipitate. However, it can be found from the figure that the conversion of LFP to $FePO_4$ can be directly realized according to the yellow arrow path under a certain acid concentration and redox potential, realizing the selective leaching of lithium ions [31].

In this paper, a combination of traditional leaching and selective leaching methods was proposed. In the early stage, when the initial acid concentration was 0.4 mol·L^{-1} (pH = 0.398), partial lithium and ferrous ions were leached out. At this time, ozone could preferentially oxidize the leached ferrous ions in the solution. After a certain amount of acid was consumed, the pH of the solution was maintained in the range of 2 and 3. Since the oxidation–reduction potential of ozone under an acidic environment is 2.07 eV, which is higher than the oxidation potential of LFP, the ferrous ion in LFP could be directly oxidized. Therefore, it can be verified that the selective leaching of lithium ions from LFP could be realized by the HCl-ozone system from the perspective of thermodynamics.

Figure 8 shows that all the peaks in the XRD pattern of the raw material are in good agreement with those in the pattern of LFP with the standard orthorhombic metaolivine structure (PDF#40-1499); the unit cell parameters are a = 0.6019 nm, b = 1.0347 nm, and c = 0.4704 nm. The XRD pattern of the leaching residue is similar to that of the original cathode material, and corresponds to the crystalline orthogonal $FePO_4$ phase (PDF#34-0134). The unit cell parameters of the leaching residue are a = 0.5824 nm, b = 0.923 nm, and c = 0.4786 nm. These

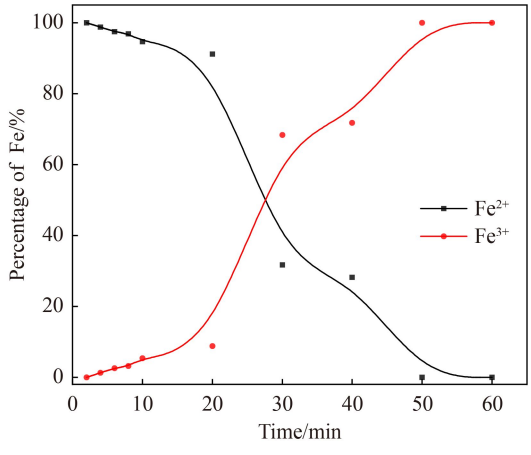

Fig. 6 Amounts of Fe^{2+} and Fe^{3+} in solution at different times during leaching process.

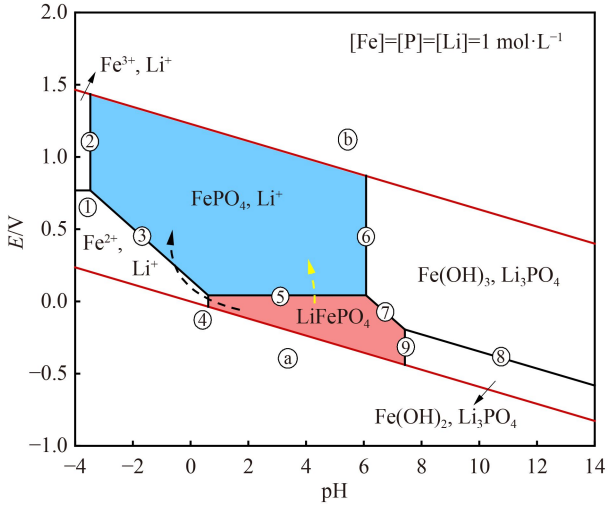

Fig. 7 E-pH diagram of the Li–Fe–P–H_2O system and the relationship between the electrode potential of redox couples and pH (25 °C).

results show that the lattice structure of LFP was basically the same before and after leaching, and LFP underwent *in situ* selective leaching of lithium in an HCl-ozone environment. The XRD patterns of the leaching residues at different reaction times show that the leaching residues at 4 and 8 min are mainly consisted of mixed crystals of LFP and $FePO_4$. The positions of the (020), (120), (211), and (131) crystal planes shifted to the right, and the unit cell constants became smaller. These results are consistent with those reported in the literature [37]. They show that in the rapid lattice oxidation leaching stage, i.e., at 0–20 min, HCl and ozone directly oxidized LFP to $FePO_4$. Lithium was leached into the solution. The XRD pattern of the leaching residue at 30 min corresponds to that of $FePO_4$. This is consistent with the composition of the leaching residue at 60 min. This shows that the residual LFP in the solution was mainly oxidized within 30–60 min, and all of it was eventually converted to $FePO_4$.

During the LFP leaching process, the Fe^{2+} was almost completely converted to Fe^{3+}. The Fe 2p XPS peak was used to verify the oxidation states of iron before and after leaching. Figure S6 (cf. ESM) shows the Fe 2p photon energy spectrum. Because of spin−orbit coupling, the Fe 2p spectrum contains two components (Fe 2p3/2 and Fe 2p1/2). The binding energy of the main peak are related to the valence state of Fe. The Fe 2p3/2 and Fe 2p1/2 peaks from divalent Fe in LFP are located at 710.5 and 724 eV, respectively. The main Fe 2p3/2 and Fe 2p1/2 peaks from trivalent Fe in $FePO_4$ are located at 712.5 and 726 eV, respectively. These results are consistent with literature reports of the Fe valence changes during the charging and discharging of LFP [38]. After leaching for 4 min, the amount of Fe^{3+} in the leaching residue began to decrease, and the characteristic peak of Fe^{3+} appeared; at 30 min, the Fe^{3+} in the crystal had basically all been oxidized to Fe^{3+}. The XPS spectrum at 60 min of leaching is almost the same as that at 30 min, which indicates that the Fe^{2+} in the LFP lattice has been completely oxidized to Fe^{3+}. These results are consistent with the XRD results.

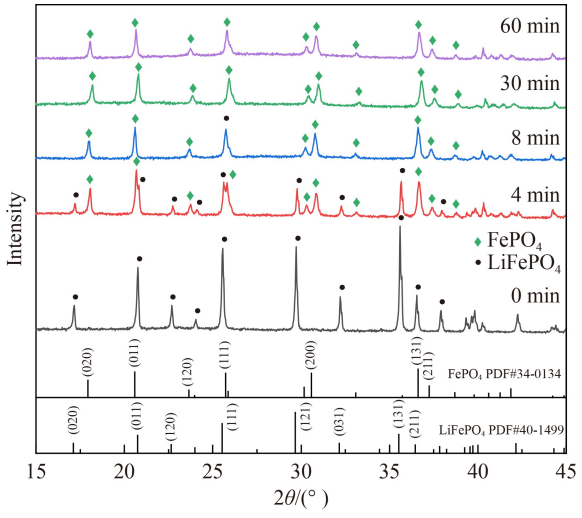

Fig. 8 XRD analyses of various solids.

The materials were examined by SEM before and after leaching; the images are shown in Fig. S7 (cf. ESM). The SEM images show that the particles of the LFP are of uniform size, which indicates smoothness. The particles of the material after leaching, i.e., $FePO_4$, are agglomerated and the surface is rougher. However, the basic particle morphology is unchanged. The SEM results were confirmed by performing particle size analysis of the materials before and after leaching; the results are shown in Fig. S8 (cf. ESM), which shows that the LFP particle size before leaching was mainly in the range 0.1–1.0 μm, and the D_{50} was 0.26 μm. The $FePO_4$ leaching residue particle size was in the range 1.5–5 μm, and the D_{50} was 2.49 μm. This indicates agglomeration of particles in the $FePO_4$ leaching residue.

In summary, during leaching, LFP was selectively leached *in situ* under the action of HCl and ozone, and the crystal structure did not change during leaching. The leaching process can be divided into two parts: fast leaching and slow leaching. In the fast leaching process, the divalent Fe in the LFP crystal lattice was quickly and directly oxidized to trivalent Fe, and lithium was leached into the solution. In the slow leaching process, which occurred at 30–60 min, oxidation of the divalent Fe in the solution was completed, and the iron remained in the leaching residue in the form of $FePO_4$.

3.8 LFP powder recycling

Based on the above results, a new recycling process for LFP cathode material was proposed (Fig. 9). The LFP powder was treated under the following conditions: 20 °C, 0.4 mol·L^{-1} HCl, Li:H (mol/mol) = 1:1, ozone concentration 10 ± 1 mg·L^{-1}, and ozone flow rate 1.5 L·min^{-1}. After leaching for 60 min, the lithium

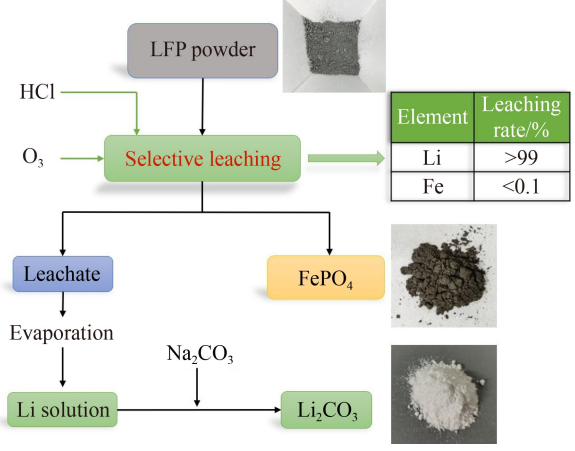

Fig. 9 Proposed lithium recovery process of LFP cathode materials.

leaching yield was greater than 99%, and the iron leaching yield was 0.07%. The filtered lithium leachate contained no other impurity ions, therefore crystallization did not occur during concentration. After concentration of the leachate, the pH was adjusted to remove traces of leached iron, and Na_2CO_3 was used to precipitate Li_2CO_3 of purity 99.9%. The filter residue was mainly olivine-type $FePO_4$, which could be used for the preparation of new LFP cathode materials.

4 Conclusions

In this study, the impact of by-products on subsequent lithium product recovery was mitigated by using ozone as the oxidant in the recovery of LFP powder. A process was developed for the selective recovery of lithium from LFP cathode materials. The conclusions obtained are as follows.

(1) The experimental results showed that the optimal operating conditions were 0.4 $mol \cdot L^{-1}$ HCl, Li:H (mol/mol) = 1:1, ozone concentration 10 ± 1 $mg \cdot L^{-1}$, and ozone flow rate 1.5 $L \cdot min^{-1}$. After leaching at 20 °C for 60 min, the lithium and iron leaching yields were 98.81% and 0.07%, respectively.

(2) Lithium was recovered from the filtrate after leaching. The primary yield of lithium precipitation was 89%, and the purity of the obtained Li_2CO_3 product was 99.9%, which matches the quality of battery-grade Li_2CO_3. The leaching residue consisted of $FePO_4$ and had a good olivine structure. It provided a good precursor for LFP electrode materials.

(3) Selective leaching of lithium from LFP was achieved by using a combination of HCl and ozone. The main function of HCl was to provide an acidic environment for the oxidant; ozone has a high redox potential and can oxidize divalent Fe in LFP to trivalent Fe *in situ* in an acidic environment, and the lithium was leached into the solution.

Based on the above results, a process for selective recovery of lithium from LFP powder was proposed. This process was developed by quantitatively studying the selective leaching of lithium in LFP on the basis of the chemical reaction equation. The developed method achieved rapid and efficient selective leaching of lithium at room temperature. More importantly, ozone can be prepared *in situ* with air or oxygen as the raw material, and the decomposition product is oxygen. Compared with the traditional hydrometallurgy methods, using ozone as an oxidant has the advantages of nearly no introduction of additional impurity ions, low dosage of chemical reagents, no discharge of high-salt wastewater. The proposed recovery method achieved rapid and efficient selective leaching of lithium ions at room temperature, which has a broad range of potential applications.

Acknowledgements This work was supported by the National Natural Science Foundation of China (Grant Nos. 22125802, and 22078010), Beijing Natural Science Foundation (Grant No. 2222017) and Big Science Project from BUCT (Grant No. XK180301). The authors gratefully acknowledge these grants. We thank Helen McPherson, PhD, from Liwen Bianji (Edanz), for editing the English text of a draft of this manuscript.

Electronic Supplementary Material Supplementary material is available in the online version of this article at https://dx.doi.org/10.1007/s11705-022-2261-0 and is accessible for authorized users.

References

1. Shen W, Han W J, Wallington T J, Winkler S L. China electricity generation greenhouse gas emission intensity in 2030: implications for electric vehicles. Environmental Science & Technology, 2019, 53(10): 6063–6072
2. Dunn J B, Gaines L, Kelly J C, James C, Gallagher K G. The significance of Li-ion batteries in electric vehicle life-cycle energy and emissions and recycling's role in its reduction. Energy & Environmental Science, 2015, 8(1): 158–168
3. Richa K, Babbitt C W, Gaustad G, Wang X. A future perspective on lithium-ion battery waste flows from electric vehicles. Resources, Conservation and Recycling, 2014, 83(1): 63–76
4. Chen X P, Li J Z, Kang D Z, Zhou T, Ma H R. A novel closed-loop process for the simultaneous recovery of valuable metals and iron from a mixed type of spent lithium-ion batteries. Green Chemistry, 2019, 21(23): 6342–6352
5. Wang Y Q, An N, Wen L, Wang L, Jiang X T, Hou F, Yin Y X, Liang J. Recent progress on the recycling technology of Li-ion batteries. Journal of Energy Chemistry, 2021, 55(4): 391–419
6. Yu H J, Zhang T Z, Yuan J, Li C D, Li J M. Trial study on EV battery recycling standardization development. Advanced Materials Research, 2013, 610-613: 2170–2173
7. Wang W, Wu Y F. An overview of recycling and treatment of spent $LiFePO_4$ batteries in China. Resources, Conservation and Recycling, 2017, 127: 233–243
8. Harper G, Sommerville R, Kendrick E, Driscoll L, Slater P, Stolkin R, Walton A, Christensen P, Heidrich O, Lambert S, Abbott A, Ryder K, Gaines L, Anderson P. Recycling lithium-ion batteries from electric vehicles. Nature, 2019, 575(7781): 75–86
9. Omar H, Rohani S. Treatment of landfill waste, leachate and landfill gas: a review. Frontiers of Chemical Science and Engineering, 2015, 9(1): 15–32
10. Hu J T, Zhang J L, Li H X, Chen Y Q, Wang C Y. A promising approach for the recovery of high value-added metals from spent lithium-ion batteries. Journal of Power Sources, 2017, 351(31): 192–199
11. Sun Z H I, Xiao Y, Sietsma J, Agterhuis H, Yang Y. A cleaner process for selective recovery of valuable metals from electronic waste of complex mixtures of end-of-life electronic products. Environmental Science & Technology, 2015, 49(13): 7981–7988
12. Zou H Y, Gratz E, Apelian D, Wang Y. A novel method to recycle mixed cathode materials for lithium ion batteries. Green Chemistry, 2013, 15(5): 1183–1191
13. Barik S P, Prabaharan G, Kumar L. Leaching and separation of

Co and Mn from electrode materials of spent lithium-ion batteries using hydrochloric acid: laboratory and pilot scale study. Journal of Cleaner Production, 2017, 147(20): 37–43

14. He L P, Sun S Y, Yu J G. Performance of $LiNi_{1/3}Co_{1/3}Mn_{1/3}O_2$ prepared from spent lithium-ion batteries by a carbonate co-precipitation method. Ceramics International, 2018, 44(1): 351–357
15. Yaug L, Xi G X, Xi Y B. Recovery of Co, Mn, Ni, and Li from spent lithium ion batteries for the preparation of $LiNi_xCo_yMn_zO_2$ cathode materials. Ceramics International, 2015, 41(9): 11498–11503
16. Song X, Hu T, Liang C, Long H L, Zhou L, Song W, You L, Wu Z S, Liu J W. Direct regeneration of cathode materials from spent lithium iron phosphate batteries using a solid phase sintering method. RSC Advances, 2017, 7(8): 4783–4790
17. Xu B, Dong P, Duan J G, Wang D, Huang X S, Zhang Y J. Regenerating the used $LiFePO_4$ to high performance cathode via mechanochemical activation assisted V^{5+} doping. Ceramics International, 2019, 45(9): 11792–11801
18. Yao Y L, Zhu M Y, Zhao Z, Tong B H, Fan Y, Hua Z. Hydrometallurgical processes for recycling spent lithium-ion batteries: a critical review. ACS Sustainable Chemistry & Engineering, 2018, 6(11): 13611–13627
19. Wang L H, Li J, Zhou H M, Huang Z Q, Tao S D, Zhai B K, Liu L Q, Hu L S. Regeneration cathode material mixture from spent lithium iron phosphate batteries. Journal of Materials Science Materials in Electronics, 2018, 29(11): 9283–9290
20. Ku H, Jung Y, Jo M, Park S, Kim S, Yang D, Rhee K, An E M, Sohn J, Kwon K. Recycling of spent lithium-ion battery cathode materials by ammoniacal leaching. Journal of Hazardous Materials, 2016, 313(5): 138–146
21. Zhao Z W, Si X F, Liu X H, He L H, Liang X X. Li extraction from high Mg/Li ratio brine with $LiFePO_4/FePO_4$ as electrode materials. Hydrometallurgy, 2013, 133: 75–83
22. Lv W G, Wang Z H, Cao H B, Sun Y, Zhang Y, Sun Z. A critical review and analysis on the recycling of spent lithium-ion batteries. ACS Sustainable Chemistry & Engineering, 2018, 6(2): 1504–1521
23. Li H, Xing S Z, Liu Y, Li F J, Guo H, Kuang G. Recovery of lithium, iron, and phosphorus from spent $LiFePO_4$ batteries using stoichiometric sulfuric acid leaching system. ACS Sustainable Chemistry & Engineering, 2017, 5(9): 8017–8024
24. Jing Q K, Zhang J L, Liu Y B, Yang C, Ma B Z, Chen Y Q, Wang C Y. E-pH diagrams for the Li−Fe−P−H_2O system from 298 to 473 K: thermodynamic analysis and application to the wet chemical processes of the $LiFePO_4$ cathode material. Journal of Physical Chemistry C, 2019, 123(23): 14207–14215
25. Zhang J L, Hu J T, Liu Y B, Jing Q K, Yang C, Chen Y Q, Wang C Y. Sustainable and facile method for the selective recovery of lithium from cathode scrap of spent $LiFePO_4$ batteries. ACS Sustainable Chemistry & Engineering, 2019, 7(6): 5626–5631
26. Liu K, Tan Q Y, Liu L L, Li J H. Acid-free and selective extraction of lithium from spent lithium iron phosphate batteries via a mechanochemically induced isomorphic substitution. Environmental Science & Technology, 2019, 53(16): 9781–9788
27. Dai Y, Xu Z D, Hua D, Gu H N, Wang N. Theoretical-molar Fe^{3+} recovering lithium from spent $LiFePO_4$ batteries: an acid-free, efficient, and selective process. Journal of Hazardous Materials, 2020, 396(5): 122707
28. Yang Y X, Meng X Q, Cao H B, Lin X, Liu C M, Sun Y, Zhang Y, Sun Z. Selective recovery of lithium from spent lithium iron phosphate batteries: a sustainable process. Green Chemistry, 2018, 20(13): 3121–3133
29. Li L, Lu J, Zhai L Y, Zhang X X, Curtiss L, Jin Y, Wu F, Chen R J, Amine K. A facile recovery process for cathodes from spent lithium iron phosphate batteries by using oxalic acid. CSEE Journal of Power and Energy Systems, 2018, 4(2): 219–225
30. Li H Y, Ye H, Sun M C, Chen W J. Process for recycle of spent lithium iron phosphate battery via a selective leaching-precipitation method. Journal of Central South University, 2020, 27(11): 3239–3248
31. Qiu X J, Zhang B C, Xu Y L, Hu J G, Deng W T, Zou G Q, Hou H S, Yang Y, Sun W, Hu Y H, Cao X, Ji X. Enabling the sustainable recycling of $LiFePO_4$ from spent lithium-ion batteries. Green Chemistry, 2022, 24(6): 2506–2515
32. Khadre M A, Yousef A E, Kim J G. Microbiological aspects of ozone applications in food: a review. Journal of Food Science, 2001, 66(9): 1242–1252
33. Behera S S, Parhi P K. Leaching kinetics study of neodymium from the scrap magnet using acetic acid. Separation and Purification Technology, 2016, 160: 59–66
34. Jin H, Zhang J L, Wang D D, Jing Q K, Chen Y G, Wang C Y. Facile and efficient recovery of lithium from spent $LiFePO_4$ batteries via air oxidation-water leaching at room temperature. Green Chemistry, 2022, 24(1): 152–162
35. Shentu H J, Xiang B, Cheng Y J, Dong T, Gao J, Xia Y G. A fast and efficient method for selective extraction of lithium from spent lithium iron phosphate battery. Green Chemistry, 2021, 23(11): 2506–2515
36. Yang L M, Feng Y F, Wang C G, Fang D F, Yi G P, Gao Z, Shao P H, Liu C L, Luo X B, Luo S L. Closed-loop regeneration of battery-grade $FePO_4$ from lithium extraction slag of spent Li-ion batteries via phosphoric acid mixture selective leaching. Chemical Engineering Journal, 2022, 431(8): 133232
37. Ramana C, Mauger A, Gendron F, Julien C, Zaghib K. Study of the Li-insertion/extraction process in $LiFePO_4/FePO_4$. Journal of Power Sources, 2009, 187(2): 555–564
38. Castro L, Dedryvere R, El Khalifi M, Lippens P E, Bréger J, Tessier C, Gonbeau D. The spin-polarized electronic structure of $LiFePO_4$ and $FePO_4$ evidenced by in-lab XPS. Journal of Physical Chemistry C, 2010, 114(41): 17995–18000